

# Two-color mixing for classifying agricultural products for safety and quality

Fujian Ding, Yud-Ren Chen, Kuanglin Chao, and Diane E. Chan

We show that the chromaticness of the visual signal that results from the two-color mixing achieved through an optically enhanced binocular device is directly related to the band ratio of light intensity at the two selected wavebands. A technique that implements the band-ratio criterion in a visual device by using two-color mixing is presented here. The device will allow inspectors to identify targets visually in accordance with a two-wavelength band ratio. It is a method of inspection by human vision assisted by an optical device, which offers greater flexibility and better cost savings than a multispectral machine vision system that implements the band-ratio criterion. With proper selection of the two narrow wavebands, discrimination by chromaticness that is directly related to the band ratio can work well. An example application of this technique for the inspection of carcasses chickens of afflicted with various diseases is given. An optimal pair of wavelengths of 454 and 578 nm was selected to optimize differences in saturation and hue in CIE LUV color space among different types of target. Another example application, for the detection of chilling injury in cucumbers, is given, here the selected wavelength pair was 504 and 652 nm. The novel two-color mixing technique for visual inspection can be included in visual devices for various applications, ranging from target detection to food safety inspection. © 2006 Optical Society of America

OCIS codes: 330.1730, 330.1880, 330.1400.

## 1. Introduction

Spectroscopy methods and multispectral imaging and hyperspectral imaging techniques have been applied for detection of military-targets, assessments of natural resources, and detection of diseases, defects, and contamination for food safety and quality. The Instrumentation and Sensing Lab (ISL) of the U. S. Department of Agriculture applies these technologies to the safety inspection of agricultural products.<sup>1-6</sup> The band ratio, which is the ratio of reflectance intensities at two different wavelengths, is invariant to geometric and illumination changes in the environment and thus is a good criterion for target discrimination. It is used in digital image processing to enhance the contrast between selected features and

superfluous features. The band-ratio criterion has been used effectively in some applications.<sup>7-13</sup>

Band-ratio analyses are conducted with multispectral imaging systems, which generally use several beams of light separated by a beam splitter, with bandpass filters of different wavelengths and two or more CCD optical sensors, as shown in Fig. 1(a). One calculates a band ratio by dividing the intensity values of pixels in the image at one waveband by the intensity values of corresponding pixels in the image of another waveband.

To detect diseases or contamination in agricultural products, the band-ratio criterion is often used in multispectral machine vision systems to enhance the separation between wholesome and diseased or contaminated products. However, implementation of multispectral imaging systems can be complicated and expensive. For some small meat and poultry plants, a low-cost visual device that can be used in existing environment conditions is preferred.

At the ISL, Ding *et al.* are developing low-cost, optically enhanced visual-sensor devices to assist inspectors or plant processors in small meat and poultry plants to conduct inspections *in situ*.<sup>14</sup> One design for an inspection assistance device based on the band-ratio criterion consists of a binocular device equipped with a special two-narrowband interference optical

---

The authors are with the Instrumentation and Sensing Laboratory, Henry A. Wallace Beltsville Agricultural Research Center, Agricultural Research Service, U.S. Department of Agriculture, Building 303, BARC-East, 10300 Baltimore Avenue, Beltsville, Maryland 20705. Y.-R. Chen's e-mail address is chen@ba.ars.usda.gov.

Received 23 November 2004; revised 3 May 2005; accepted 5 May 2005.

0003-6935/06/040668-10\$15.00/0

© 2006 Optical Society of America

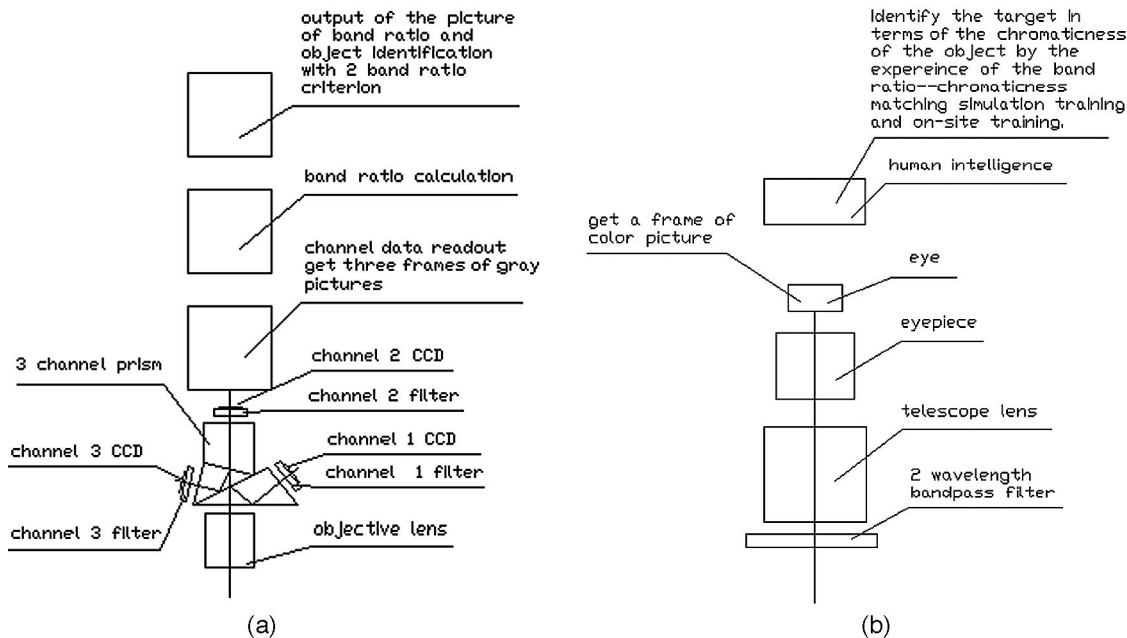


Fig. 1. Schematic of implementation of the band-ratio criterion: (a) with a multispectral imaging System and (b) with a two-color mixing visual device.

filter, which would satisfy several requirements of *in situ* inspection. First, color extraction can easily be obtained. Second, angular resolution and brightness are sufficient to permit inspection of objects at a distance. Third, with the small field of view of the binoculars, an interference filter can easily be implanted in an optical system. Fourth, this optical device would be much less expensive and more portable than a multispectral imaging system.

Using optimized illuminating sources is often an ideal approach in certain applications.<sup>15,16</sup> For a slaughter plant environment in which controlled lighting is often impractical, however, it is preferable to use the existing illuminating sources of fluorescent lamps. This application aims to develop a wearable visual device that can utilize band-ratio criteria without relying on controlled narrowband illuminating sources. Using an optically enhanced binocular device, small plant operators could be able to detect defective, diseased, and contaminated poultry carcasses at a distance by identifying colors corresponding to specific carcass conditions as a result of the selected band-ratio criterion, without using specifically optimized illumination.

In this paper we establish the relationship between color attributes of colors perceived through optical two-color mixing and the band-ratio of the two wave bands and demonstrates its application for food safety inspection. The color attributes of the mixture of the two wave bands are shown to be directly related to the reflectance ratio between the two wave bands in a particular lighting environment. This technique of visually perceiving the band ratio through optical color mixing is useful not only for developing food safety inspection tools but also for target detection and quality inspection in other fields.

## 2. Relationship between Color Attributes and the Band-Ratio Criterion

When an optical system is used for viewing object color, the tristimulus values  $X$ ,  $Y$ ,  $Z$  of an object color are given as follows:<sup>17</sup>

$$\begin{aligned} X &= k \sum_{\lambda} \tau_{\lambda} \rho_{\lambda} H_{\lambda} \bar{x}_{\lambda} \Delta\lambda, \\ Y &= k \sum_{\lambda} \tau_{\lambda} \rho_{\lambda} H_{\lambda} \bar{y}_{\lambda} \Delta\lambda, \\ Z &= k \sum_{\lambda} \tau_{\lambda} \rho_{\lambda} H_{\lambda} \bar{z}_{\lambda} \Delta\lambda, \end{aligned} \quad (1)$$

where  $\bar{x}_{\lambda}$ ,  $\bar{y}_{\lambda}$ , and  $\bar{z}_{\lambda}$  are 1931 CIE color-matching functions,  $k$  is a normalizing factor  $H_{\lambda} \Delta\lambda$  is the spectral distribution of the flux irradiating the object,  $\rho_{\lambda}$  is the spectral reflectance of the object, and  $\tau_{\lambda}$  is the transmittance of the optical system.

If two colors with tristimulus values  $(X_1, Y_1, Z_1)$  and  $(X_2, Y_2, Z_2)$  and chromaticity coordinates  $(x_1, y_1, z_1)$  and  $(x_2, y_2, z_2)$  are mixed, a new color is produced that has chromaticity coordinates  $(x_m, y_m, z_m)$  that can be expressed as follows:

$$\begin{aligned} x_m &= (k_1 x_1 + x_2) / (k_l + 1), \\ y_m &= (k_1 y_1 + y_2) / (k_l + 1), \\ z_m &= (k_1 z_1 + z_2) / (k_l + 1), \end{aligned} \quad (2)$$

where  $k_l$  is expressed as

$$k_l = (X_1 + Y_1 + Z_1) / (X_2 + Y_2 + Z_2). \quad (3)$$

The chromaticity coordinates  $(x_m, y_m, z_m)$  will remain constant if  $k_l$  remains constant. The intensity after mixing is the luminance,  $Y_m$ , which is equal to the sum of  $Y_1$  and  $Y_2$ . In this application the  $(x_1, y_1, z_1)$  and  $(x_2, y_2, z_2)$  values are for narrowband light signals through narrowband interference filters and thus are independent of changes in illumination and surface reflectance.

The band ratio,  $C_{br}$ , of the intensities at  $\lambda_1$  and  $\lambda_2$  can be expressed as follows:

$$C_{br} = E_{\lambda_1}/E_{\lambda_2}, \quad (4)$$

$$E_{\lambda_1} = \int_{\lambda_1 - \Delta\lambda_1/2}^{\lambda_1 + \Delta\lambda_1/2} F' \tau_{\lambda}' \rho_{\lambda} H_{\lambda}' S_{\lambda} d\lambda,$$

$$E_{\lambda_2} = \int_{\lambda_2 - \Delta\lambda_2/2}^{\lambda_2 + \Delta\lambda_2/2} F' \tau_{\lambda}' \rho_{\lambda} H_{\lambda}' S_{\lambda} d\lambda, \quad (5)$$

where  $E_{\lambda_1}$  and  $E_{\lambda_2}$  represent the energy in the unit time received by the optical sensor at  $\lambda_1$  and  $\lambda_2$ , respectively,  $F'$  is the geometrical function for a given optical system,  $\tau_{\lambda}'$  is the spectral transmission of the optical system,  $H_{\lambda}'$  is the spectral energy of the lighting source for a specified integration time,  $S_{\lambda}$  is the spectral responsivity of the optical sensor, and  $\lambda_1$  and  $\lambda_2$  are the central wavelengths of the narrow wavebands. As  $F'$  is the same for the different wavelength bands,  $C_{br}$  can be expressed as follows:

$$C_{br} = \frac{\int_{\lambda_1 - \Delta\lambda_1/2}^{\lambda_1 + \Delta\lambda_1/2} \tau_{\lambda}' \rho_{\lambda} H_{\lambda}' S_{\lambda} d\lambda}{\int_{\lambda_2 - \Delta\lambda_2/2}^{\lambda_2 + \Delta\lambda_2/2} \tau_{\lambda}' \rho_{\lambda} H_{\lambda}' S_{\lambda} d\lambda}. \quad (6a)$$

In most applications, bandwidths  $\Delta\lambda_1$  and  $\Delta\lambda_2$  are small enough that the band ratio can be expressed as follows:

$$C_{br} = \tau_{\lambda_1}' \rho_{\lambda_1} H_{\lambda_1}' S_{\lambda_1} \Delta\lambda_1 / (\tau_{\lambda_2}' \rho_{\lambda_2} H_{\lambda_2}' S_{\lambda_2} \Delta\lambda_2). \quad (6b)$$

Equation (6b) shows that the band ratio is independent of the geometrical function and that, for a given system, the band ratio is only a function of the relative reflectance of the object, if the illuminating condition remains constant. It can be concluded that the band ratio,  $C_{br}$ , is not sensitive to the variation of the intensity of illumination with a stable spectrum, not sensitive to the objective distance between the optical system and the objects, and not sensitive to the angle between the optical axis and the normal line of the object surface.

By allowing inspectors to visually perceive differences enhanced by the band-ratio criterion, color-mixing optical devices present an extremely useful tool to inspectors for whom an enhanced ability to separate wholesome from diseased or contaminated

products is important. In this section the relationship between the band-ratio criterion and target color attributes is given. Using the CIE LUV color space,<sup>17</sup> we define the color difference between two targets as follows:

$$\Delta E(L^*u^*v^*) = [(\Delta L^*)^2 + (\Delta u^*)^2 + (\Delta v^*)^2]^{1/2}. \quad (7)$$

Also, the saturation and hue,  $s_{uv}^*$  and  $h_{uv}$ , respectively, of a single target are defined as

$$s_{uv}^* = 13[(u' - u_n')^2 + (v' - v_n')^2]^{1/2}, \quad (8)$$

$$h_{uv} = \arctan(v^*/u^*). \quad (9)$$

When bandwidths  $\Delta\lambda_1$  and  $\Delta\lambda_2$  are equal and small, Eq. (3) and (6b) can be used to give  $k_l$  as follows:

$$k_l = \frac{\tau_{\lambda_1} \tau_{\lambda_2}' H_{\lambda_1} H_{\lambda_2}' S_{\lambda_2} (\bar{x}_{\lambda_1} + \bar{y}_{\lambda_1} + \bar{z}_{\lambda_1})}{\tau_{\lambda_2} \tau_{\lambda_1}' H_{\lambda_2} H_{\lambda_1}' S_{\lambda_1} (\bar{x}_{\lambda_2} + \bar{y}_{\lambda_2} + \bar{z}_{\lambda_2})} C_{br} \quad (10a)$$

or

$$k_l = c_1 C_{br}, \quad (10b)$$

where the parameter  $c_1$  remains constant. The saturation and hue can be obtained as follows:

$$s_{uv}^* = \{[a_1(C_{br} + a_2)^2 + a_3]/(C_{br} + a_4)^2\}^{1/2}, \quad (11)$$

$$h_{uv} = \arctan[b_1/(C_{br} + b_2) + b_3], \quad (12)$$

where  $(x_n, y_n, z_n)$  are the chromaticity coordinates of the reference white point and the parameters of  $a_1, a_2, a_3, a_4, b_1, b_2,$  and  $b_3$  are functions of the chromaticity coordinates  $(x_1, y_1, z_1), (x_2, y_2, z_2), (x_n, y_n, z_n)$  and  $c_1$  (see Appendix A). For a specific target and viewing condition, the chromaticity coordinates  $(x_1, y_1, z_1), (x_2, y_2, z_2),$  and  $(x_n, y_n, z_n)$  are constants, so the parameters of  $a_1, a_2, a_3, a_4, b_1, b_2,$  and  $b_3$  are all constants. Therefore  $s_{uv}^*$  and  $h_{uv}$  are only functions of  $C_{br}$ . With the formulations of Eq. (11) and (12), the saturation and the hue of a perceived object color can be calculated from its band ratio. So, in this application, we can determine the respective color attributes in terms of band ratio for use in the food safety inspection. The color attributes can be used in color simulation for training inspectors to recognize and differentiate between chromaticities of different targets under various conditions.

The exact relation between the band-ratio criterion and the parameters  $s_{uv}^*$  and  $h_{uv}$  can be expressed as follows:

$$C_{br} = \frac{1}{c_1} \left[ \frac{d_1 + d_2 s_{uv}^* \cos(h_{uv})}{d_3 + d_4 s_{uv}^* \cos(h_{uv})} \right], \quad (13)$$

where  $d_1, d_2, d_3,$  and  $d_4$  are constants determined by  $(x_1, y_1, z_1), (x_2, y_2, z_2),$  and  $(x_n, y_n, z_n)$  (see Appen-

dix A). Equation (13) shows that target detection by band ratio is directly related to the color chromaticness of the color that results from two-band mixing. Equation (13) can be used to calculate the band ratio that corresponds to the color attributes, including saturation and hue. According to Eq. (11)–(13), the relation between band ratio and color attributes (saturation and hue) is one to one.

For any case in which the two-wavelength band-ratio criterion is effective, the visual method will also work. Any given combination of saturation and hue is an indicator of a specific target condition or object. With Eqs. (11)–(13), a specific saturation and hue can be determined from any given two-waveband ratio or can be used to calculate the corresponding two-waveband ratio.

### 3. Example Applications of Two-Color Mixing for Safety Inspection of Food and Agricultural Products

In recent years, U.S. consumers have increased their consumption of poultry products. To ensure a safe and wholesome supply of poultry products for consumers, U.S. legislation requires U.S. Department of Agriculture Food Safety and Inspection Service inspectors at poultry slaughter plants to inspect every carcass to be sold for consumption. These experienced inspectors visually and manually inspect the carcass's exterior, the inner surfaces of the body cavity, and the visceral organs for apparent diseases and defects.

Septicemia–toxemia (septo), a systemic disease condition, is the most common cause of carcass condemnation (removal of a bird from the processing line). Septicemia is caused by pathogenic microorganisms or their toxins in the bloodstream, whereas toxemia refers to a condition in which the blood contains toxins either produced by cells at a localized infection or derived from the growth of microorganisms. Carcasses with septo are often dark red to bluish in color, dehydrated, stunted, or edematous.<sup>18</sup> The other conditions that most commonly cause removal from the processing line are airsacculitis (a lung disease) and tumors (cartilaginous nodules). Inspectors also condemn carcasses for other defects that are not associated with any diseases, such as cadaver (resulting from improper slaughter), bruises, inflammatory processes (IPs), and fecal contamination. These unwholesome carcass conditions are characterized by a variety of obvious changes in skin color.

Figure 1(b) shows a schematic of an optical device that uses the band-ratio criterion for assisting in poultry inspection. Low cost  $8 \times 32$  binoculars with  $7.5^\circ$  fields of view are equipped with special two-wavelength bandpass filters. An interference dual-bandpass filter can be installed in the front of the binoculars with a custom-made filter holder. The spectral transmission of the dual-bandpass filter is shown in Fig. 2.

All the results are based on the conditions that the optical transmissions of the visual device and the multispectral system are similar in the visible range and that the spectral energy distribution of the illu-

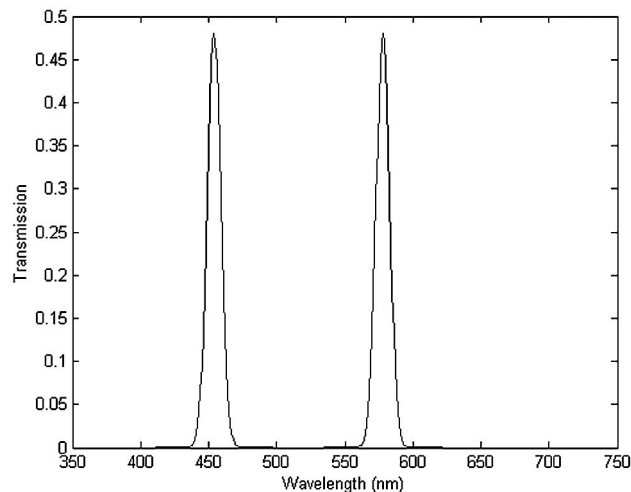


Fig. 2. Spectral transmission of the two-narrow-band interference filter.

minating sources in the multispectral system application and the visual device application comply with the standard for a CIE D65 illuminating source as in many slaughter plants.

#### A. Optimal Wavelength Pair for Identification of Object Conditions

##### 1. Selection of Optimal Wavelength Pair for the Identification of Chicken Carcass Conditions

A total of 467 chicken carcasses (213 wholesome, 51 airsacculitis, 80 cadaver, 51 IP, 64 septo, and 8 tumor) were obtained from a processing line at a poultry slaughter plant at Cordova, Maryland. The wholesome and unwholesome conditions were identified in the plant by U.S. Department of Agriculture Food Safety and Inspection Service inspectors. Chicken carcasses were marked according to condition and placed in plastic bags to minimize dehydration during transport. Then the bags were placed in coolers, covered with ice, and transported to the ISL facility in Beltsville, Maryland, within 2 h of removal from the processing line.

For each sample, the right breast was removed with the skin intact, and from this a 49 mm diameter circular area was cut out. The skin, approximately 4 mm thick, was removed and set aside while the meat was sliced to a thickness of 15 mm. Before sample reflectance measurements were taken, dark background and white reference [black and white poly (tetrafluoroethylene), respectively] measurements were collected. For a sample reflectance measurement, the sample (chicken meat with skin overlaid) was placed in a sample holder, and a fiber-optic probe was positioned 2 cm above the surface of the sample.

Visible–near-infrared reflectance spectra were collected by use of a photodiode array spectrophotometer (Oriel Company, Stratford, Conn.) in the wavelength range 411.0–923.0 nm, in increments of 0.5 nm, resulting in 1024 data points per spectrum. To improve the signal-to-noise ratio, each spectrum was the

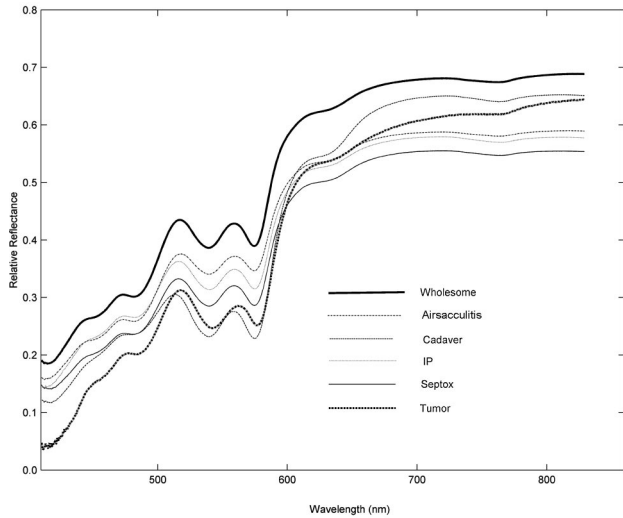


Fig. 3. Relative reflectances of chicken samples.

average of 244 scans of the diode array, where each scan was a result of a 0.0328 s photodiode array exposure.

Figure 3 shows relative reflectance spectra of various chicken carcass conditions. Searching for optimal wavelengths for the visual device to use in identifying the chicken conditions is an important step; in particular, the process must take into account human vision and its perception of color, because not all band-ratio wavelength pairs used in the multispectral system are suitable for use in a visual device. Here the criterion used for searching is the chromaticness difference, in term of saturation and hue  $\Delta S' = 13[(\Delta u')^2 + (\Delta v')^2]^{0.5}$ .

Because it is necessary to identify each of the six poultry conditions in a multitarget (multiple unwholesome conditions) application, the objective of optimization of the waveband pair is to select the waveband pair that has the maximum  $\Delta S'_{\lambda_1\lambda_2}$ , which means the smallest differences in chromaticness be-

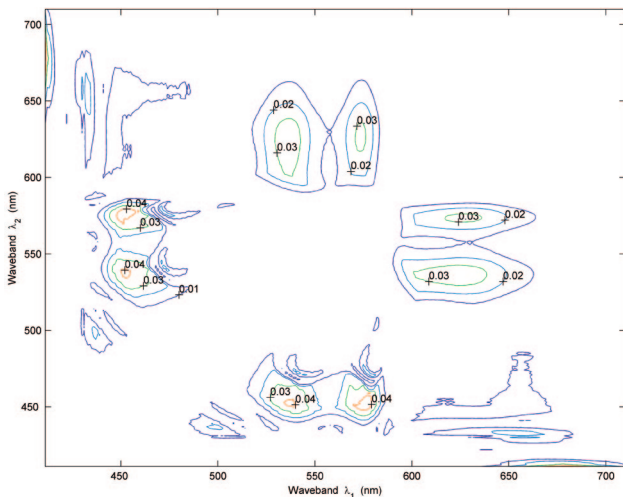


Fig. 4. (Color online) Contour plot of minimum chromaticness difference  $\Delta S'_{\lambda_1\lambda_2}$  for multitarget detection.

Table 1. Waveband Pairs Selected with Chromaticness Difference Index ( $\Delta S'$ )

Target Condition	Wavelength (nm)	
	Band 1	Band 2
Multitarget	454	578
Single-target		
Wholesome	449	571
Airsacculitis	441	576
Cadaver	462	575
IP	454	591
Septicemia	509	628
Tumor	431	501

tween different conditions of chicken carcasses at the waveband pair  $(\lambda_1, \lambda_2)$ . After the waveband pair is selected, the color differences between different conditions of chicken carcasses are used to check whether the waveband pair obtained by the  $\Delta S'_{\lambda_1\lambda_2}$  criterion is useful in this application.

Figure 4 shows plots of  $\Delta S'_{\lambda_1\lambda_2}$  values for all possible waveband combinations (90,000 waveband pairs) for multitarget detection. Four areas of peak  $\Delta S'_{\lambda_1\lambda_2}$  values occur near the  $(\lambda_1, \lambda_2)$  waveband pairs of (454, 578 nm), (452, 537 nm), (624, 538 nm), and (627, 574 nm) for which the  $\Delta S'_{\lambda_1\lambda_2}$  values are 0.0467, 0.0412, 0.0355, and 0.0320, respectively. The waveband pair of (454, 578 nm) has the highest  $\Delta S'_{\lambda_1\lambda_2}$  value and is a potential selection for multitarget detection when the color differences are large enough. The wavelengths with the largest chromaticness differences and enough color difference for single-target

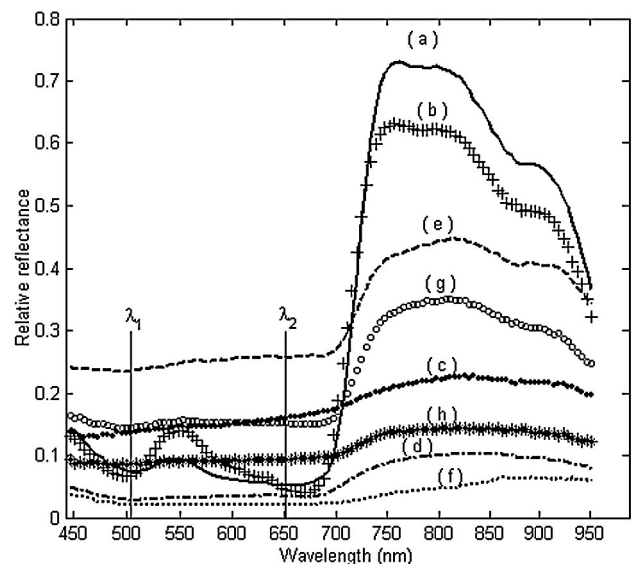


Fig. 5. Relative reflectance of chilling injury in cucumbers: (a) Good-smooth skins of green color, (b) good-smooth skins of yellow color, (c) chilling-injured skins of gray color, (d) chilling-injured skins of black color, (e) chilling-injured skins of white color, (f) chilling-injured skins of black color, (g) chilling-injured skins of gray color, (h) and chilling-injured skins of gray color.

**Table 2. Saturation and Band Ratio at Wavelength Pair 454 and 578 nm**

Target Condition	$C_{br}$	$k_1$	$S_{UV}^*$
Wholesome	0.3959	0.9856	0.5397
Airsacculitis	0.3812	0.9491	0.5872
Cadaver	0.4956	1.2337	0.2407
IP	0.4270	1.0631	0.4421
Septicemia	0.4120	1.0256	0.4888
Tumor	0.3625	0.9026	0.6490

detection and for multitarget detection are listed in Table 1.

**2. Selection of Optimal Wavelength Pair for the Detection of Chilling Injury in Cucumbers**

Cucumbers and a variety of other vegetables are sensitive to low temperatures. Overexposure to low-temperature environments can induce chilling-injury symptoms that include pitting, discoloration, internal browning, and decay. Symptoms of chilling injury develop rapidly and can become sites for further fungal decay and bacterial infection once the exposure to cold is followed by a few days at warmer temperatures. Bacterial pathogens may then be transmitted to human beings through consumption of uncooked or mishandled vegetables. Thus, one of the greatest concerns in the vegetable industry is the detection of chilling injury.

Commercially ready cucumbers were picked at a farm near Beltsville, Maryland, during the 2002 harvest season. Only cucumbers that were free from damage according to visual inspection were used for the study. Forty-five cucumbers were randomly subdivided into fifteen groups of three cucumbers each, and their hyperspectral images were collected before cold storage treatment. Each group was placed in a plastic bag perforated with holes to allow for air circulation, and all 15 bags were placed in a dark and temperature-controlled cold room at 0 °C for chilling treatment. Over a period of 15 days, one bag was removed each day and placed in an air-conditioned laboratory room (room temperature, 18–20 °C) for postchilling storage. Each day at room temperature, hyperspectral images were collected not only for the three cucumbers removed that day but also for all cucumbers removed during previous days. The last group was removed to room temperature after 15

days of cold storage, and daily room temperature imaging continued for the following 6 days.

A hyperspectral imaging system developed by the ISL was used to scan the cucumbers in line-scan operation with an incrementally controlled precision positioning table. For each line scan, image data of 460 (spatial pixels) × 112 (spectral bands) were collected. The spectral wavelength range was 447–951 nm, with 4.5 nm intervals. Two 150 W halogen lamps provided the illumination for image collection. A white Spectralon panel with a nearly 99% reflection ratio was used as a reference.

Data for the group of cucumbers stored for 12 days at 0 °C were used for the selection of wavelength pairs. Regions of interest (ROIs) were chosen from areas of (a) good smooth skins of green color; (b) good smooth skins of yellow color; (c) chilling-injured skins of gray color; (d) chilling-injured skins of black color; (e) chilling-injured skins of white color; (f) chilling-injured skins of black color; (g) chilling-injured skins of gray color; and (h) chilling injured skins of gray color. The relative reflectances of skins with these conditions are shown in Fig. 5. Given the color variations that are evident for both good and injured skin, the selection of a waveband pair for detecting chilling injury was aimed at minimizing the chromaticness difference between good smooth skins while maximizing the chromaticness differences between chilling-injury skins and good skins.

To facilitate detection of all the variations of conditions for chilling-injured areas, the waveband pair is selected that has the maximum  $\Delta S_{\lambda_1\lambda_2}'$ , which is the smallest chromaticness difference between different conditions of good skins and different chilling-injury skins at the waveband pair  $(\lambda_1, \lambda_2)$ . After the waveband pair is selected, the color differences between different conditions of cucumbers are used to check whether the waveband pair obtained by the  $\Delta S_{\lambda_1\lambda_2}'$  criterion is appropriate in this application.

**B. Viewing Device and Lighting**

Because the existing illuminating sources that are already present in many poultry slaughter plants are similar to the CIE D65 standard source, a D65 source was used in this study for appropriate adaptation of the visual device. The objects were illuminated with 5000 Lx of light from a D65 source, the adaptation was 20% of the luminance of white in the adapting field, and only light passing through the binoculars' special filters

**Table 3. Multitarget Color Difference with Two Wavebands, 454 and 578 nm**

Target Condition	Wholesome	Air-Sacculitis	Cadaver	IP	Septicemia	Tumor
Wholesome	0.0	3.57	26.5	10.7	11.0	11.9
Airsacculitis		0.0	25.9	10.4	9.66	8.36
Cadaver			0.0	15.8	16.4	24.6
IP				0.0	2.97	12.2
Septicemia					0.0	9.60
Tumor						0.0

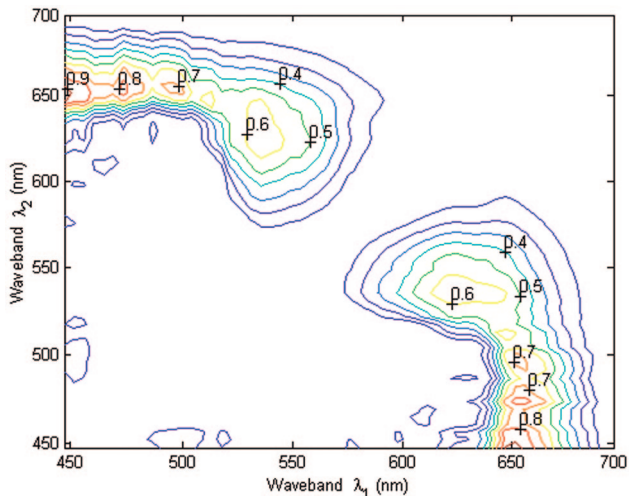


Fig. 6. (Color online) Contour plot of minimum chromaticness difference  $\Delta S_{\lambda_1\lambda_2}'$  between good skin and chilling-injured skin.

reached the viewer. The white color seen through this device is different from the D65 color, so we finish the color simulation with the condition that white is D65 with an adapting field luminance of  $18 \text{ cd/m}^2$ , using the revision of CIE color appearance model CIECAM97s proposed by Fairchild,<sup>19</sup> which can be used to convert from tristimulus values to perceptual attributes, while the inverse model can be used to convert from perceptual attributes to tristimulus values. The input and output viewing conditions are used during the forward and inverse calculations to account for differences in viewing conditions.

#### 4. Results and Discussion

##### A. Applications for Food Safety Inspection of Chicken Carcasses

Table 2 lists the saturation and band-ratio values. Because the reference white point is illuminating light through the visual device, all the hues for the various conditions are  $84.99^\circ$ . The resultant color dif-

Table 4. Band Ratios of Several ROIs of Cucumber Skins at Wavelength Pair 504 and 652 nm

ROIs <sup>a</sup>	Band Ratio in Our Multispectral System
Good smooth skin	
(a)	0.5482
(b)	0.5708
Chilling-injury skin	
(c)	0.3454
(d)	0.3939
(e)	0.3451
(f)	0.3032
(g)	0.3203
(h)	0.3570

<sup>a</sup>See Fig. 5 for definitions of ROIs (a)–(h).

Table 5. Color Differences between Chilling-Injury Skins and Good Smooth Skins with Two Wavebands, 504 and 652 nm<sup>a</sup>

Chilling-Injury Skins	Good Smooth Skins	
	(a)	(b)
(c)	36.3687	30.8647
(d)	30.9247	24.5731
(e)	39.3947	35.3469
(f)	22.8964	17.7021
(g)	28.8168	23.9406
(h)	26.3202	20.2060

<sup>a</sup>See Fig. 5 for definitions of ROIs (a)–(h).

ferences among the various conditions are listed in Table 3.

If the color difference is greater than 5.0, it is considered to be easily differentiable by eye for a large target, whereas a color difference of 1.0 is considered to be color difference only noticeable under the CIE reference viewing condition.<sup>20</sup> From Table 3 we conclude that, with 454 and 578 nm mixing, the normal carcass condition can easily be separated from all the defective and diseased conditions, with the lowest color difference of 3.57 for separation from the airsacculitis condition. Cadaver and tumorous conditions are most easily separated from other conditions,

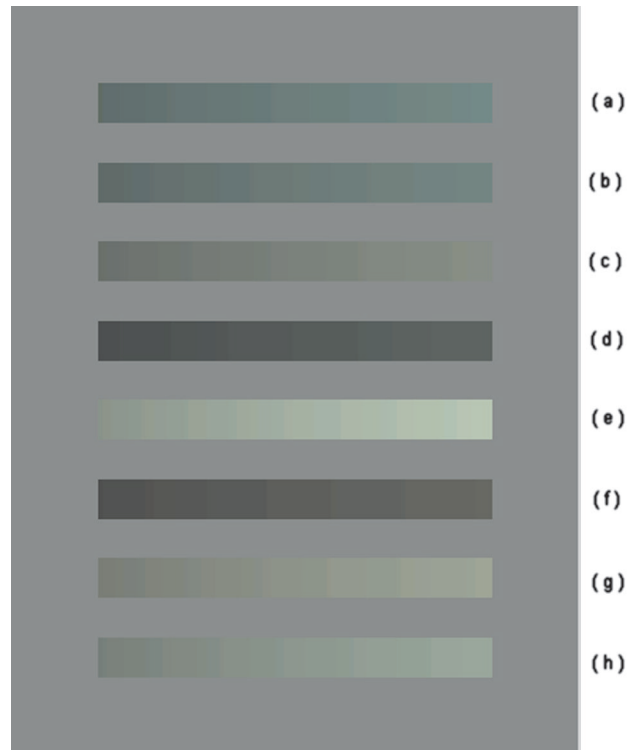


Fig. 7. Training chromaticity chart for chilling injury: (a) good smooth skins of green color, (b) good-smooth skins of yellow color, (c) chilling-injured skins of gray color, (d) chilling-injured skins of black color, (e) chilling-injured skins of white color, (f) chilling-injured skins of black color, (g) chilling-injured skins of gray color, (h) chilling-injured skins of gray color.

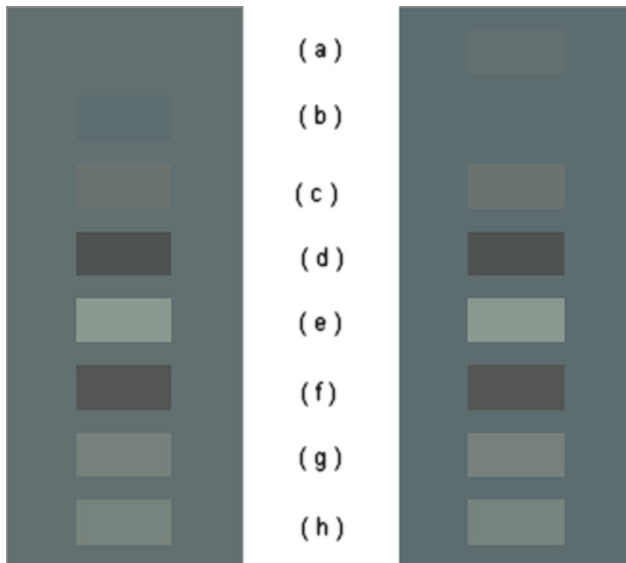


Fig. 8. Training color chart for chilling injury: (a) good smooth skins of green color, (b) good smooth skins of yellow color, (c) chilling-injured skins of gray color, (d) chilling-injured skins of black color, (e) chilling-injured skins of white color, (f) chilling-injured skins of black color, (g) chilling-injured skins of gray color, (h) chilling-injured skins of gray color.

and the septox condition can easily be separated from normal, airsacculitis, and cadaver conditions. But the septox condition is not so easily separated from the IP condition; there is a noticeable color difference of only 2.97.

#### B. Applications for Detection of Chilling Injury of Cucumbers

With the criterion of  $\Delta S_{\lambda_1\lambda_2}$ , an ideal wavelength pair, 504 and 652 nm, was found as shown in Fig. 6, which shows a plot of the minimum  $\Delta S_{\lambda_1\lambda_2}$  values between the smooth good skins and different kinds of chilling-injury skins for all possible waveband combinations ( $112 \times 112$  waveband pairs) for chilling-injury detection.

The band ratios of the ROIs in our multispectral system with the D65 illuminating source are listed in Table 4. The band ratios of the good smooth skin are 0.5482 and 0.5708, corresponding to ROIs of (a) green good smooth skin and (b) yellow good smooth skin. The band ratios of the chilling-injury skins are 0.3454, 0.3939, 0.3451, 0.3032, 0.3203, and 0.3570, corresponding to ROIs of areas (c), (d), (e), (f), (g), and (h). It is obvious that there is a remarkable band-ratio difference between good smooth skin and the chilling-injury skin at the wavelength pair of 504 and 652 nm. Because the band-ratio difference between the various good smooth skins is small, the different backgrounds, including green smooth skin and yellow good smooth skin, have almost the same chromaticity. Thus chilling-injured skins are easily detected compared with areas of good smooth skins in term of chromaticness.

With the wavelength pair of 504 and 652 nm, a training color chart was developed to allow an inspec-

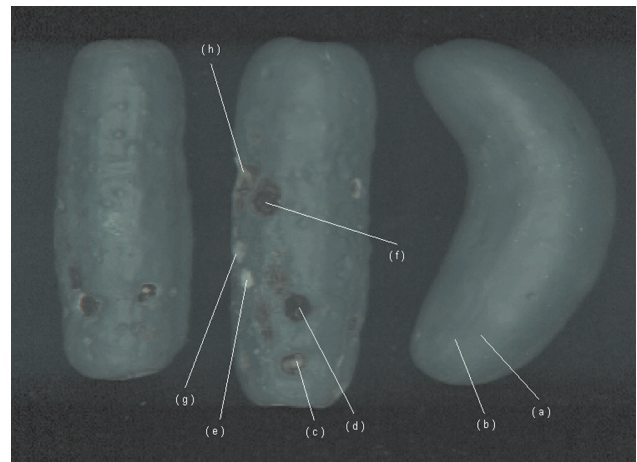


Fig. 9. Simulated picture of one group of chilling-injured cucumbers: (a) good smooth skin of green color, (b) Good smooth skin of yellow color, (c) chilling-injured skin of gray color, (d) chilling-injured skin of black color, (e) chilling-injured skin of white color, (f) chilling-injured skin of black color, (g) chilling-injured skins of gray color, (h) chilling-injured skin of gray color.

tor to gain familiarity with the colors of the different conditions of good smooth skins and chilling-injury skins. The color differences between ROIs of good smooth skins and those of chilling-injury skins are greater than 17, as given in Table 5. The chilling injury areas are easily detected by use of wavelength pair of 504 and 652 nm.

In Fig. 7 every color bar has the same chromaticity along its length but a different brightness, corresponding to the respective band-ratio conditions of the cucumber skins. The reflective intensity of cucumber skin increases from 60% to 150%, progressing from left to right on each bar, relative to the average reflective intensity of the respective cucumber skins. Using this color chart, farm operators can learn the band ratios that correspond to different cucumber skins in terms of two-color perceptual attributes, saturation and hue. Then they can determine where the chilling-injury skins are. The left-hand side of Fig. 8 represents the green-color good smooth skin background, and the right-hand side represents the yellow-color good smooth skin background. From the color chart of the backgrounds of both green smooth skin and yellow good skin, the different chilling-injury skins are easily detected because of the obvious chromaticness differences between the background good skins and the target skins. In Fig. 9, a simulated color appearance model image of the cucumbers is shown. The chromaticness differences among different good smooth skins are small, whereas differences between chilling-injury skins and good skins are obvious. Thus it is feasible to detect cucumber chilling injury by using this device. In Fig. 9 all the chilling-injury skins, including ROIs of all different colors, have such obvious chromaticness differences from the good skins that it is easy to detect the chilling-injury skins. At the same time, all

the other chilling-injury skins outside the ROIs have been detected easily.

## 5. Conclusions

In food safety and quality inspection it is important to have systems or devices that can help to separate wholesome products effectively from diseased or defective ones. Spectroscopic band ratios are powerful tools for discriminating among two or multiple classes. In this paper we have presented a visual method of implementing the band ratio criterion. Using a two-band-filter optical device, we related the extracted color to the band-ratio at two narrow wavebands. With this method an inspector can identify the target in accordance with the band-ratio criterion.

A formulation that includes saturation, hue, and a two-wavelength band ratio has been presented. The saturation and hue that correspond to different band-ratio conditions of chicken carcasses were given. Further, it was demonstrated that the differences in the resultant mixed color among wholesome and diseased and defective chicken carcasses are large enough to be used for discrimination. According to the example of detection of chilling injury of cucumbers, it was shown that this visual method can easily identify the different conditions of chilling injury. From the above examples of application, this kind of visual method can be used in classifying food and agricultural products for safety and quality. It was shown that it is feasible to develop a low-cost, binocular-based inspection device that will assist operators at small slaughter and processing plants to detect defective, diseased, and contaminated carcasses accurately at a distance with enough angular resolution. The two-color mixing technique can greatly improve the separation power of visual inspection. Also, it can be used in visual or binocular devices that are useful for other target detection as long as the band-ratio criterion works in the visible wavelength range.

### Appendix A. Derived Relationship among

$a_{1-4}$ ,  $b_{1-3}$ ,  $d_{1-4}$ , and  $(x_1, y_1, z_1)$ ,  $(x_2, y_2, z_2)$ , and  $(x_n, y_n, z_n)$

$$g_1 = 4x_1$$

$$g_2 = 4x_2$$

$$g_3 = x_1 + 15y_1 + 3z_1$$

$$g_4 = x_2 + 15y_2 + 3z_2$$

$$g_5 = 4x_n / (x_n + 15y_n + 3z_n)$$

$$g_6 = 9y_1$$

$$g_7 = 9y_2$$

$$g_8 = 9y_n / (x_n + 15y_n + 3z_n)$$

$$e_1 = g_1/g_3 - g_5$$

$$e_2 = g_2/g_3 - g_1 g_4/g_3^2$$

$$e_3 = g_4/g_3$$

$$e_4 = g_6/g_3 - g_8$$

$$e_5 = g_7/g_3 - g_6 g_4/g_3^2$$

$$a_1 = 169(e_1^2 + e_4^2)$$

$$a_2 = (e_1^2 e_3 + e_1 e_2 + e_4^2 e_3 + e_4 e_5) / [c_1(e_1^2 + e_4^2)]$$

$$a_3 = 169[e_1^2 e_3^2 + 2e_1 e_2 e_3 + e_2^2 + e_4^2 e_3^2 + 2e_3 e_4 e_5 + e_5^2 - (e_1^2 e_3 + e_1 e_2 + e_4^2 e_3 + e_4 e_5)^2 / (e_1^2 + e_4^2)] / c_1^2$$

$$a_4 = e_3/c_1$$

$$b_1 = [(g_7 - g_4 g_8) / (g_1 - g_3 g_5) - (g_2 - g_4 g_5)(g_6 - g_3 g_8) / (g_1 - g_3 g_5)^2] / c_1$$

$$b_2 = (g_2 - g_4 g_5) / [c_1(g_1 - g_3 g_5)]$$

$$b_3 = (g_6 - g_3 g_8) / (g_1 - g_3 g_5)$$

$$d_1 = g_4 g_5 - g_2$$

$$d_2 = g_4/13$$

$$d_3 = g_1 - g_3 g_5$$

$$d_4 = -g_3/13$$

The authors thank Xuemei Zhang, Agilent Technologies, Inc.; Michael D'Zmura, University of California, Irvine; and Noboru Ohta, Munsell Color Science Laboratory, Rochester Institute of Technology, for their kind suggestions.

Mention of a product or specific equipment does not constitute a guarantee or warranty by the U.S. Department of Agriculture and does not imply its approval to the exclusion of other products that may also be suitable.

### References

1. Y. R. Chen, K. Chao, and M. S. Kim, "Machine vision technology for agricultural applications," *Comput. Electron. Agr.* **36**, 173–191 (2002).
2. Y. R. Chen, W. R. Hruschka, and H. Early, "On-line trials of a chicken carcass inspection system using visible/near-infrared reflectance," *J. Food Process Eng.* **23**, 89–99 (2000).
3. Y. R. Chen and D. R. Massie, "Visible/NIR reflectance and interactance spectroscopy for detection of abnormal poultry carcasses," *Trans. ASAE* **36**, 863–869 (1993).
4. Y. R. Chen, "Classifying diseased poultry carcasses by visible and near-IR reflectance spectroscopy," in *Optics in Agriculture and Forestry*, J. A. De Shazer and G. E. Meyer, ed., *Proc. SPIE* **1836**, 44–55 (1992).
5. K. Chao, Y. R. Chen, W. R. Hruschka, and F. B. Gwozdz, "On-line inspection of poultry carcasses by dual-camera system," *J. Food Eng.* **51**, 185–192 (2002).

6. M. S. Kim, A. M. Lefcourt, and Y. R. Chen, "Multispectral laser-induced fluorescence imaging system for large biological samples," *Appl. Opt.* **42**, 3927–3934 (2003).
7. M. M. Abdeen, A. K. Thurmond, M. G. Abdelsalam, and R. J. Stern, "Application of ASTER band-ratio images for geological mapping in arid regions: the neoproterozoic Allaqi Suture, Egypt," presented at the Annual Meeting of the Geological Society of America, 5–8 November 2001.
8. J. C. Volesky, R. J. Stern, and M. G. Abdelsalam. "Mineral exploration with LANDSAT ETM+ and ASTER data in the Wadi Bidah mineral district, Saudi Arabia," presented at the Annual Meeting of the Geological Society of America, 5–8 November 2001.
9. A. M. Lefcourt, M. S. Kim, and Y. R. Chen, "Automated detection of fecal contamination of apples by multispectral laser-induced fluorescence imaging," *Appl. Opt.* **42**, 3935–3943 (2003).
10. P. M. Mather, *Computer Processing of Remotely Sensed Imagery* (Wiley, 1987).
11. P. M. Mather, *Computer Applications in Geography* (Wiley, 1991).
12. N. M. Short, Processing and classification of remotely sensed data; pattern recognition; approaches to data/image interpretation," [http://rst.gsfc.nasa.gov/Intro/Part2\\_6.html](http://rst.gsfc.nasa.gov/Intro/Part2_6.html).
13. Y. Liu and Y. R. Chen, "Analysis of visible reflectance spectra of stored, cooked and diseased chicken meats," *Meat Sci.* **58**, 395–401 (2001).
14. F. Ding, Y. R. Chen, and K. Chao, "Two-waveband color-mixing binoculars for the detection of wholesome and unwholesome chicken carcasses: a simulation," *Appl. Opt.* **44**, 5454–5462 (2005).
15. M. Vriesenga, G. Healey, J. Sklansky, and K. Peleg, "Colored illumination for enhancing discriminability in machine vision," *J. Vis. Commun. Image Represent.* **6**, 244–255 (1995).
16. N. Tsumura, T. Tanaka, H. Haneishi, and Y. Miyake, "Optimal design of mosaic color filters for the improvement of image quality in electronic endoscopes," *Opt. Commun.* **145**, 27–32 (1998).
17. G. Wyszecki and W. S. Stiles, *Color Science: Concepts and Methods, Quantitative Data and Formulas* (Wiley, 1982).
18. B. P. Dey, Y. R. Chen, C. Hsieh, and D. E. Chan, "Detection of septicemia in chicken livers by spectroscopy," *Poultry Sci.* **82**, 199–206 (2003).
19. M. D. Fairchild, "Revision of CIECAM97s for practical applications," *Color Res. Appl.* **26**, 418–427 (2001).
20. International Commission on Illumination, *Recommendation on Uniform Color Spaces, Color Difference Equations, Psychometric Color Terms*, Suppl. 2 to CIE Publ. 15 (E.-1.3.1), 1971/ (TC-1.3.) (Commission Internationale de l'Éclairage, 1978).